C. R. Physique 17 (2016) 524–532

Contents lists available at ScienceDirect

Comptes Rendus Physique

www.sciencedirect.com

Phononic crystals / Cristaux phononiques

Acoustic metamaterials for sound mitigation

Métamatériaux acoustiques pour l'isolation sonique

Badreddine Assouar [a,b,*], Mourad Oudich [a,b], Xiaoming Zhou [a,b,c]

[a] *CNRS, Institut Jean-Lamour, 54506 Vandœuvre-lès-Nancy, France*
[b] *University of Lorraine, Institut Jean-Lamour, bd des Aiguillettes, BP 70239, 54506 Vandœuvre-lès-Nancy, France*
[c] *Key Laboratory of Dynamics and Control of Flight Vehicle, Ministry of Education and School of Aerospace Engineering, Beijing Institute of Technology, Beijing 100081, China*

ARTICLE INFO

Article history:
Available online 17 February 2016

Keywords:
Acoustic metamaterials
Phononics
Acoustic propagation
Sound mitigation

ABSTRACT

We provide theoretical and numerical analyses of the behavior of a plate-type acoustic metamaterial considered in an air-borne sound environment in view of sound mitigation application. Two configurations of plate are studied, a spring-mass one and a pillar system-based one. The acoustic performances of the considered systems are investigated with different approaches and show that a high sound transmission loss (STL) up to 82 dB is reached with a metamaterial plate with a thickness of 0.5 mm. The physical understanding of the acoustic behavior of the metamaterial partition is discussed based on both air-borne and structure-borne approaches. Confrontation between the STL, the band structure, the displacement fields and the effective mass density of the plate metamaterial is made to have a complete physical understanding of the different mechanisms involved.

RÉSUMÉ

Dans ce travail, nous présentons des études théoriques et numériques sur le comportement physique de métamatériaux acoustiques en plaque dans un environnement sonique dans le but de développer des systèmes pour l'isolation acoustique. Deux configurations sont analysées, une à base d'un système masse-ressort et une à base d'un système à piliers. Les performances acoustiques des systèmes en question ont été étudiées suivant différentes approches et ont montré l'obtention d'une perte en transmission (STL) allant jusqu'à 82 dB pour un métamatériau en plaque ayant une épaisseur de 0.5 mm. L'interprétation physique des performances acoustiques de ces métamatériaux est analysée à la base des deux approches sonique et vibratoire considérées dans ce travail. Une confrontation entre les résultats des pertes en transmission, la structure de bande, les champs de déplacement et la densité de masse effective du métamatériau est réalisée afin de comprendre les mécanismes physiques mis en jeu.

* Corresponding author at: CNRS, Institut Jean-Lamour, 54506 Vandœuvre-lès-Nancy, France. Tel.: +33 (0)3 83 68 49 05.
E-mail address: Badreddine.Assouar@univ-lorraine.fr (B. Assouar).

http://dx.doi.org/10.1016/j.crhy.2016.02.002
1631-0705/

1. Introduction

For many decades, we have been witnessing an increasing demand for suppressing undesirable air noise for human comfort as well as mechanical vibrations in solid structures such as buildings, planes, and machinery in general. In fact, noise reduction is one of the key issues for enhancing the quality of life. A better night rest results in more productivity during the day, lower noise levels preserve the human ear for a longer time, and less annoyance by acoustic noise results in a better well-being in general. These issues are even more important nowadays due to the overwhelming presence of road and air traffic noise. As a matter of fact, people exposed to repetitive long periods of high level sound noise can cause health issues such as stress, sleep disorder, and even mental health problems. It is the case, for example, of industrial manufacturers working near noisy machines, aircraft passengers setting close the plane engines, or people leaving in dwelling places near heavy traffic flow roads, railway lines or airports. A higher noise level can even cause deafness in some cases. The danger of noise is not less than the one of mechanical vibration for the human body where health problems can also occur in the case of long-period direct contact with vibrating systems such as jackhammers. The low-frequency mechanical vibrations present also a real and challenging issue that the industry faces, which causes the deterioration of machines and increases significantly the maintenance coasts. In general, the combination of vibration intensity with its duration characterizes the risk in all these application fields for both acoustic and elastic noise/vibration.

Nowadays, a large research community is using the best of their scientific knowledge and means to take up the challenge of controlling acoustic and elastic waves to face all technological requirements. Sound mitigation and structure vibrations damping are important topics in acoustical and mechanical engineering. We are witnessing the development of new engineered materials and technologies to achieve high-performance mitigation for both sound and mechanical vibrations for a wide range of applications. In fact, material insulators such as foams, concrete walls, fibrous materials and rubbers are often used to increase noise absorption, sound transmission loss, and/or vibration damping. They can be found for example in buildings, especially dwelling places located near noisy environment like airports or highways. In addition, industrial manufacturers often use these specific materials to create soundproof enclosures for machinery and noisy equipment pieces as well as to reduce mechanical vibrations to avoid factor weakening. In the aerospace field, for instance, there is an increasing demand for the development of sound insulators, vibration dampers, and new technologies for aircrafts and spacecraft. In a plane, for example, continuous noises in the cabin are mostly generated by the engines (jet noise), the air flowing around (boundary layer noise), and the air-conditioning system, along with other sounds coming from the airplane control mechanism such as landing gear operation, hydraulic pumps, etc. For many decades, great efforts were undertaken to design and construct light-weight and cost-effective noise and vibration proofs for aerospace industry, and it is been commonly agreed that engineered panels based on foams are the most effective technological solutions used for this matter, although noise isolation for the frequency range below 500 Hz remains very weak.

In concrete terms, the concept of using a thick single homogeneous solid plate as a barrier to reduce undesirable acoustic noise and mechanical vibrations at the sonic level is limited by the mass density law. In fact, the plate has to be thicker to mitigate sound at the lower frequencies, and the problem of sound mitigation becomes even more challenging when seeking for lightweight and non-bulky solution systems. A well-known and used appropriate solution is viscoelastic materials where the elastic energy of mechanical vibrations is converted into heat by internal frictions and dissipated. Rubbers is the most used viscoelastic materials in industry and many works have been devoted to study the sound transmission loss through systems made of rubber. Porous materials and foams are also used to achieve the same goal, and are generally made of glass and polyester fibers [1]. Moreover, more complex technological designs of sound proofs have been developed such as the so-called double or sandwich panels, which are made of two thin plates “sandwiching” either a viscoelastic material [2] or a solid periodic structure [3] (Fig. a–b). They can then provide high internal damping to reduce resonant vibrations better than a single metallic plate. Sandwich panels are one of the most studied systems for sound insulation and vibration reduction, which are meant to be used especially in aircrafts and ships as they can offer high stiffness properties and low weight. Despite their multiple advantages, sandwich panels often display limited sound transmission loss because of the coincidence frequency region which can be much larger compared to single plates [4].

Another technological solution proposed for noise reduction is the micro-perforated plate (MPP) [5–8]. Well-designed holes in the panel can reduce the surface wave velocity in the vibrating structure, which can decrease the structural noise radiation into the air. Several works have dealt with MPPs or micro-perforated shells to study their sound-absorption and radiation performances for the single-layer configuration [5,6], and even multi-layer ones [7,8]. A sound transmission loss (STL) of almost 62 dB was reached based on these configurations. Although these technological solutions can increase the STL performances, multilayer panel structures are needed, which increases the total thickness and weight of the whole system.

In 2000, Liu et al. [9] proposed an unprecedented structure based on a new physical concept to open the possibility of breaking the mass density law. The system is known as acoustic metamaterial (AM) or locally resonant sonic crystal (LRSC), and gives the possibility to open acoustic band gaps at sonic frequency range using a reduced-size system. This kind of structure initiates a promising way to develop new designs of panels based on AM to achieve very high sound transmission loss while keeping the desired panel thickness. In general, AM are made of periodic distribution of low-frequency resonators basically made of a rigid core coated by a very soft material, usually a soft polymer, and arranged in a stiff hosting matrix. A wave propagating inside the system excites the low-frequency resonant modes occurring inside the AM. Due to the low stiffness of the polymer, the resonant modes can occur at wavelengths in the stiff hosting media much larger by some orders

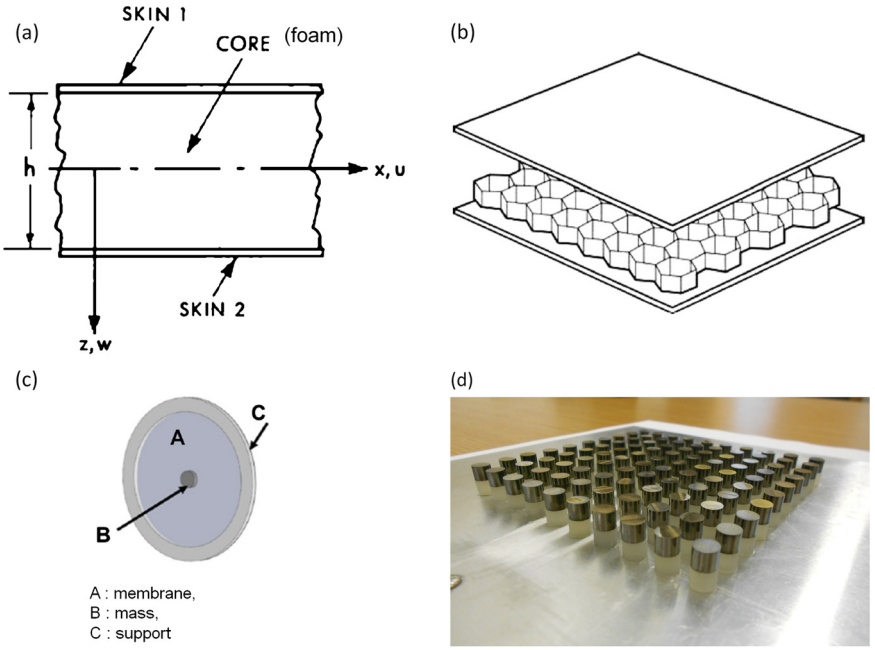

Fig. 1. Top: sandwich panel systems with either (a) foam [2] or (b) honeycomb structure [3]. Bottom: acoustic metamaterial examples [22–24].

of magnitude than the spatial impedance periodicity inside the AM. The resonant modes couple with the propagating modes in the structure to open a band gap precisely at these resonant frequencies. At this wavelength scale, the wave sees the whole structure as a homogeneous media with new physical properties, called effective properties. It was demonstrated that the AM displays high and negative values of its effective dynamic mass density at these specific resonance frequencies. The frequency range of the divergent effective mass density provides a stop band for acoustic/elastic waves inside the AM so that acoustic transmission can be significantly lowered at this frequency band. Since the pioneering works of Liu et al. [9], numerous works have demonstrated the concept of divergent negative effective mass density using AM [10–12]. Then this concept allows us to overcome the mass density law limitation and offers the possibility to create panels or partition based on AM approach to highly decrease the acoustic wave transmission without changing the system thickness.

One kind of AM plate-based which is considered as a promising solution to achieve light weight and no bulky acoustic barriers is a plate-type AM made of low-frequency resonators distributed on one side or both sides of a homogeneous elastic plate. The system is one of the most studied structures for acoustic and elastic wave prohibition in the low-frequency range [13–19]. The resonators are of cylindrical shape (pillar or stubs) and provide resonant modes at frequencies way below the Bragg scattering mechanism range fixed by the periodic distribution of the pillars. Due to the resonance of the scatterers, the AM plate produces controlled band gaps for Lamb waves [13–16] and even guiding them precisely through linear defect modes inside the structure [20–22]. Pennec et al. [13] and Wu et al. [15] were the first to introduce this kind of structure using metallic pillars on plate to demonstrate the concept of resonant gap opening for plate waves. Wu et al. [20] also provided the possibility of a wave-guiding low-frequency plate mode by introducing linear defects inside the AM plate. In the following works, instead of metallic stubs, Oudich et al. [16] used either simple soft rubber stubs or composite stub made of rubber with lead or tungsten cap, arranged on the surface of a thin aluminum plate (stubbed plate). They demonstrated that they can lower even more the resonant modes to couple with the Lamb ones (Fig. 1d). They showed that the system not only produces band gaps for Lamb waves of wavelengths at least 10 times larger than the periodicity of the structure, but also showed, both theoretically and experimentally, that the structure can confine and even guide waves, which can be interesting for energy-harvesting applications [17,21,22]. All these works were about controlling elastic wave propagation using stop bands, which makes the AM plate the more suitable for structure vibration reduction applications.

On the topic of acoustic waves propagation in air (or the so-called airborne sound approach), some studies investigated the possibility of using AM as a sound proof for noise reduction purpose. Using the impedance tube, Ho et al. [23] evaluated sound transmission through an AM plate constructed by sticking metal ball masses in thin rubber membrane units distributed on plastic rigid square grid (Fig. 1c). They demonstrated that their system can perform 96.5 dB and 86 dB STL at 630 and 250 Hz respectively, where a single perforated plate and a porous brick plate can only give STLs lower than 30 dB. In another work, Mei et al. [24] constructed an AM system composed of an elastic membrane with fixed rigid platelets capable of high airborne absorption at the sound frequency range. The system thickness is no more than 200 μm and can absorb more that 70% of the incident acoustic wave pressure at 172 Hz, whereas the wavelengths in the air are about 2 m. The physics of sound transmission through AM plates was also investigated theoretically by Xiao et al. [25]. To simplify the model, they started from AMs made of a simple thin plate supported by spring mass resonators and considered only the

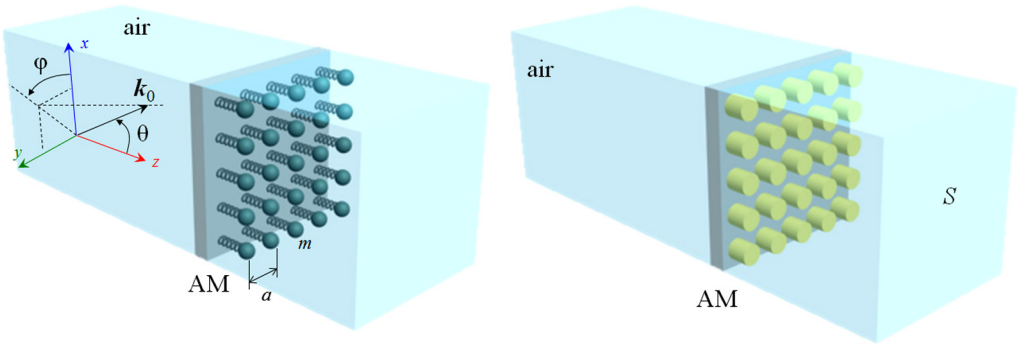

Fig. 2. Acoustic metamaterial structures in airborne sound configuration, (on the left) with spring-mass resonators, (on the right) with cylindrical pillar resonators.

flexural waves interaction with both resonators and air. They started from Kirchhoff's theory for thin plates and developed an analytical model to calculate the STL. Very recently, we gave a more general approach to calculate the STL for thick and thin plates with spring mass resonators [26].

In the present work, we provide the potential application of plate-type AM used as a sound barrier for reducing high lever sound pressure. The sound proof performances will be investigated for two AM plate examples as a proof of concept. We will first start from a simple structure made of simple spring-mass resonators distributed on an aluminum plate. The airborne sound performance of the system is evaluated using an analytical formalism based on PWE [26]. The objective is to describe and understand the physics behind high STL manifestation at the resonant frequencies. The second example will concern a more realistic structure which can be more suitable for technological applications. This second AM plate is the same as the one studied previously by the authors [17]. We recall that the system is made of aluminum plate with periodic distribution of cylindrical rubber stub and prohibits the propagation of Lamb waves at around 2 kHz. As far as we know, the airborne sound performance of such structure has never been investigated. The STL resulting from the airborne approach will be compared to the band structure so as to investigate and understand more AM plate vibrational motion modes and their interaction with the propagating sound in the air. The effective dynamic mass density was also calculated and compared to the STL results. The paper will conclude with general comments about the obtained results.

2. Acoustic metamaterial plate with spring-mass resonators

In this study, we investigate the sound transmission loss of an AM made of an aluminum plate decorated with a square array of cylindrical spring mass resonators. The airborne sound approach is considered with an incident acoustic plane wave impinging the plate having an acoustic pressure amplitude of 1 Pa (equivalent to 94 dB of the sound level). The incident wave interacts with the AM plate surface, which makes it vibrate and produce a reflected and a transmitted plane wave in the two air half spaces in contact with the AM plate. Fig. 2a gives the airborne sound transmission representation adopted in the computation where an incident wave pressure is considered with the wave vector $\vec{k}_0$. The coordinates of the latter are:

$$k_x = k_0 \sin\theta \cos\varphi$$
$$k_y = k_0 \sin\theta \sin\varphi \quad \text{and}$$
$$k_z = k_0 \cos\theta$$

where $k_0 = \omega/c_0$; c_0 is the sound velocity in the air, θ and φ are the elevation and azimuth angles, respectively, which describe the oblique incidence of the acoustic wave (Fig. 2a). The periodicity of the spring mass resonator distribution is denoted a and is fixed at 1 cm for the whole study.

To calculate the STL for the AM model in Fig. 2a, one can use the plane wave expansion method as it was described in our recent work [19]. In this example, the mass and the spring stiffness are chosen so that the resonant frequency is 2 kHz. The viscoelastic effect is considered in the spring-mass system and described with a loss factor η fixed to $\eta = 0.005$ as it is described in reference [26].

Figs. 3a and 3b present the STL results for the AM where the plate thicknesses are $h = 0.5$ mm and $h = 3$ mm, respectively. In both Figs. 3a and 3b, the solid lines in black, blue, and red correspond to STL results in the cases of a plane wave incidence with elevation angles 0, $\pi/3$ and $0.95\,\pi/2$, respectively. The three dashed lines with the same colors give the STL for a single plate without resonator (bare plate) for the same elevation angles. The asymmetric shape of observed peaks results from the Fano resonance. From both Figs. 3a and 3b, one can see that, for the AM case, a high STL value of about 75 dB can be reached at the resonance frequency (2 kHz) for incidence angles $\theta = 0$ and $\varphi = 0$ (normal incidence), while the bare plate can only give 26 dB and 42 dB for plate thicknesses of 0.5 mm and 3 mm, respectively. We can also observe that for the same frequency, AM gives high STL values of 69 dB and 52.6 dB for $\theta = \pi/3$ and $\theta = 0.95\,\pi/2$, respectively,

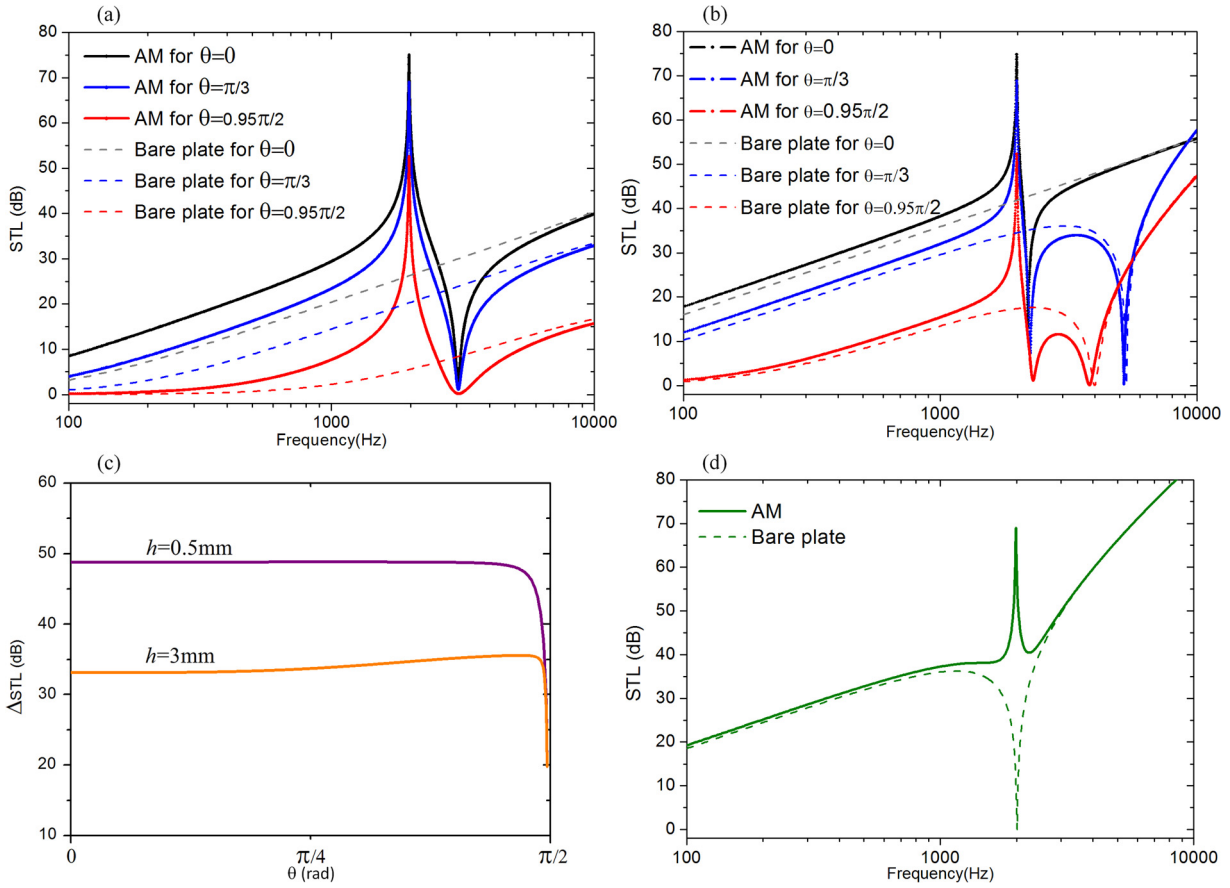

Fig. 3. Sound transmission loss curves through the metamaterial plate with square array of spring-mass resonators (period of 1 cm) on aluminum plate of thickness (a) 0.5 mm and (b) 3 mm. The STL is calculated for different incidence values of the elevation angle: normal incidence ($\theta = 0$, black solid line) and oblique for $\theta = \pi/3$ and $0.95\,\pi/2$ (blue and red solid lines, respectively). The dashed sold lines correspond to the bare plate (without resonators). (c) Difference between the STL of the AM plate and the STL of the bare plate at the resonance frequency (2 kHz) as function of the incidence angle for the cases where $h = 0.5$ mm and $h = 3$ mm. (d) STL calculation for the incident angle $\theta = \pi/3$ for the bare plate (dashed line) and the AM plate (solid line) for a plate thickness of 8 mm.

while for the bare plate only STL values of 20 dB and 5 dB are obtained for the case where $h = 0.5$ mm. The same behavior is observed for the case of plate thickness $h = 3$ mm, where the AM allows reaching STLs of 69 dB and 52 dB for $\theta = \pi/3$ and $\theta = 0.95\,\pi/2$, respectively, instead of 34.5 dB and 17 dB, obtained using only a bare plate for the same two elevation angles, respectively. To clearly evidence the comparison between the AM and the bare plate for the same thickness and for all the elevation angles, we have plotted in Fig. 3c the STL difference (ΔSTL) between the AM plate and the bare plate specifically at the resonance frequency (2 kHz) where the high STL is obtained. It is clear then that, far from the vicinity of $\theta = \pi/2$, the STL gain obtained by the AM over the bare plate is of about 50 dB and 35 dB for plate thicknesses 0.5 and 3 mm, respectively.

On the other hand, a sound loss dip of 1 dB is observed at 3 kHz for the case where $h = 0.5$ mm (2.2 kHz for $h = 3$ mm), which is associated with the resonant peak at 2 kHz. In fact, this dip does not appear in the case of the bare plate. The dip corresponds to the high transmission of the sound wave through the AM and does not depend on the elevation angle. The physics behind the presence of the pair peak and dip is the strong coupling between the resonant mode of the spring mass and the plate flexural waves. At the peak, this coupling makes the plate vibration motion vanishing at the resonance frequency as a result of wave reflection, while the dip corresponds to the situation where the plate vibration is out of phase with the mass oscillations. The peak frequency corresponds to the lower edge of the structure-borne band gap created by the AM and the dip corresponds to the upper edge of the gap [19]. At the dip's frequency, the plate vibration amplitude is enhanced, and the sound pressure amplitude is transmitted.

In the case of the plate thickness of 3 mm presented in Fig. 3b, on can also point out the existence of a second dip for both the AM and the bare plate. This dip depends on the elevation angle as it decreases from 8 to 3.9 kHz for θ ranging from $\pi/3$ to $0.95\,\pi/2$. The dip frequency is known as the coincidence frequency and corresponds to the excitation of the zero-order antisymmetric Lamb mode (flexural), which creates radiated sound waves with enhanced amplitude in the air medium. The coincidence frequency f_c is proportional to the inverse of the plate thickness and the square sin of the elevation angle θ as it is described by the formula [25]:

$$f_c(h,\theta) = \frac{1}{\pi h}\left(\frac{c_0^2}{\sin(\theta)^2}\right)\sqrt{\frac{3(1-\nu^2)\rho}{E}} \quad (1)$$

In the case where $h = 0.5$ mm, the lowest coincidence frequency is evaluated at 23.6 kHz by taking $\theta = \pi/2$, which explains its absence in the frequency range of Fig. 3a.

The coincidence frequency is one of the main limitations of panel-based systems used as sound barriers, but could be solved by using AM. In fact, we plotted in Fig. 3d the STL of the AM system where the coincidence frequency matches exactly with the resonance frequency of the spring-mass system at 2 kHz. The thickness of the plate in this case is 8 mm and the result is for $\theta = \pi/3$. The dashed line corresponds to the bare plate where one can see a dip at 2 kHz corresponding to high sound transmission caused by the plate's flexural vibration. Due to the effect of the spring mass resonators, the dip of 1 dB, observed in Figs. 3a and 3b, is completely removed and the sound loss is increased at this specific frequency to reach almost 70 dB. This example shows that it could be possible to well-design an AM plate with specific resonators having their resonant frequencies matching the coincidence frequency to overcome the plate systems limitations, which can be a promising solution for low-frequency sound mitigation.

3. Acoustic metamaterial plate with pillar resonators

The AM example in Fig. 2a is a simple case with a single resonant frequency provided by the spring-mass system and its STL performance can be easily investigated using an analytical formulation [25,26]. To be in a more realistic situation for real application, we present in this section an AM constructed by a 0.5-mm-thick plate containing cylindrical pillar resonators (Fig. 2b). The density, the longitudinal and shear wave velocities for the soft rubber are taken to be 1300 kg/m^3, 1000 m/s, and 22 m/s, respectively [27]. The structure is reported in our previous works [16–19] to have resonant modes that couple with the plate waves to open low-frequency band gaps. As the flexural waves (zero-order antisymmetric Lamb mode (A_0)) are more prone to interact with air media, particular attention will be drawn to the pillar resonant modes with mainly out-of-plane vibration (perpendicular to the plate surfaces). The reason is that these resonant modes can couple strongly with the plate mode A_0 and give then high STL values. The pillars are chosen to be in soft material, i.e. silicone rubber, so that their resonance modes occur in the sonic frequency range. In this study, we also consider the rubber viscoelastic damping by choosing a loss factor of 0.001. The latter was introduced into the model by considering a complex Young modulus for the rubber $E^* = E(1 + j\eta)$, where η is the considered loss factor. As the AM with pillars is a complicated system to be analytically investigated, we use a numerical approach based on the finite-element method to compute the acoustic performances of the structure.

Taking into account the periodicity of the AM system, we performed our calculation using only one unit supercell containing that of the AM plate as well as the air incidence and transmission media with specific periodic boundary conditions for the total wave pressure as well as the displacement field for the plate. A perfectly matched layer (PML) is used for wave attenuation to simulate the infinite incident and transmitted acoustic waves in the air and to avoid reflections in sound transmission calculation. The STL is evaluated by averaging the transmitted pressure amplitude over an air surface plane (denoted S in Fig. 2b) parallel to the plate and far from the structure by at least one wavelength. To better understand the AM plate mechanical vibrational motion behavior while interacting with the air media, we also calculated the band structure as well as the effective mass density related to the out-of-plane vibrations of the plate system. Knowing that the structure can be considered as a homogeneous media under the condition of large wavelengths compared to the AM period, the effective mass density was calculated using the finite element method by evaluating the stress resulting from specific applied displacement field on the four lateral boundaries of the plate's unit cell. Further details of the calculation method are given in reference [19].

Fig. 4 gathers the results of the band structure, the effective mass density and the STL. The left panel gives the band structure of the stubbed AM plate in the ΓX direction where the plate modes with mainly out-of-plane displacement components along the z direction are highlighted in red dots. The blue line is the sound line in the air for an oblique incidence with an elevation and azimuthal angles $\theta = \pi/4$ and $\varphi = 0$, respectively. The middle panel gives the effective dynamic mass densities ρ_{33} while the right panel presents the STL curves through the AM plate for the oblique incidence $\theta = \pi/4$ and $\varphi = 0$.

For the STL results, one can see that high peak STL denoted (α) of 82 dB is observed at 2 kHz while the associated dip denoted (α') of low STL (high sound transmission) is located at 2.54 kHz. Comparing the STL to the band structure, it is clear that the peak and the dip correspond to the band gap of the flexural waves (red shaded area), lower edge and upper edge, respectively. As a matter of fact, when an incident wave pressure interacts with the AM plate with a specific frequency corresponding to the resonance of the pillars, it excites the resonant mode, which couples with the plate vibrations and affects then sound transmission. The excited resonant modes involved are those with out-of-plane displacement (in the z direction). We also plotted in the band structure the tangential wavenumber $k_x = (\omega/c_0)\sin\theta$ line for $\theta = \pi/4$ of the incident sound wave. The intersection of the sound line curve and the mode branches in the band structure explains exactly the resonant modes observed in the STL curve. In fact, along with the mode (α), other resonant modes denoted (β) and (γ) located at 856 Hz and 2.11 kHz, respectively, appear in the STL curve by a tiny peak (see the insets which are a zoom of the STL curve). It can be then concluded that the dispersion relation can give easily a better understanding of the plate physical behavior and helps predicting the AM modes radiation through the air. Regarding the effective mass density, one

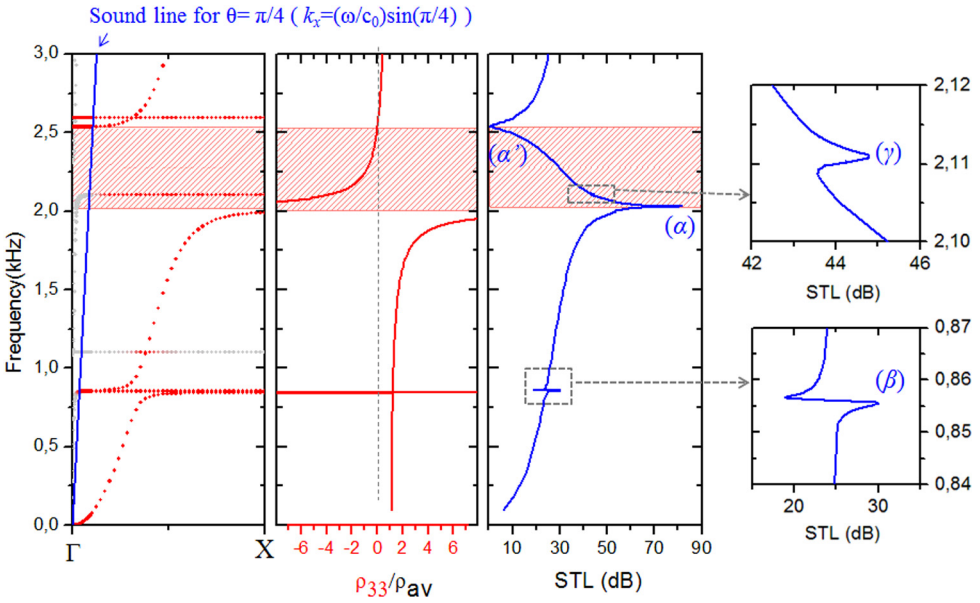

Fig. 4. Left panel. Band structure of the stubbed AMM plate in the ΓX direction, where the plate's modes with mainly out-of-plane displacement components along the z direction are highlighted in red dots. The blue line is the sound line in the air for an oblique incidence with elevation and azimuthal angles $\theta = \pi/4$ and $\varphi = 0$ respectively. Middle panel. The effective dynamic mass density is ρ_{33}. ρ_{av} is the average density of the unit cell calculated by taking into account the rubber and aluminum densities and volumes. (Right panels) STL curves through the AM plate for the oblique incidence $\theta = \pi/4$ and $\varphi = 0$.

can clearly conclude that the effective mass density component ρ_{33} becomes divergent in the gap frequency edge as it takes high values in the lower edge of the gap, and have negative value in the band gap frequency range. This proves the concept of breaking the mass density law by this type of AM at the sonic frequency range for sound insulation purposes.

We finish this paper by plotting in Fig. 5 the displacement field of the AM plate for the unit cell as well as the acoustic transmitted wave pressure at the particular modes (α), (α'), (β) and (γ). One can see that, at 2 kHz, the incident wave pressure excites the resonant mode (α) of the pillar where the vibrational motion corresponds to a successive stretching and compression of the pillar along the vertical direction z. In this case, the displacement field vanishes at the bottom of the pillar, and subsequently the displacement field of the plate disappears, so that almost no wave pressure is transmitted into the air media. However, in the upper edge of the out-of-plane gap, which corresponds to the dip (α') in the STL curve, the successive stretching and compression of the pillar are out of phase with the plate that vibrates strongly, creating a high transmitted wave into the air. More precisely, the mechanical vibrations of the plate at these two points correspond to the anti-resonance (α) and resonant (α') modes of the whole plate. The anti-resonance corresponds to a zero vibrational amplitude at the bottom of the pillar, which means low transmission by the plate through the air (STL peak), whereas the resonance corresponds to maximum of the transmission (STL dip). Moreover, regarding the excitation of the anti-resonant modes (β) and (γ) located at 856 Hz and 2.11 kHz, they undergo vibrational motion along the x and z directions. They are excited because of the oblique incidence of the sound by the continuity of the tangential wavenumber component k_x to the plate surface from the air into the AM plate. As the pillars have non-zero displacement field along the z direction for theses modes, they couple also with the A_0 mode and affect then plate interaction with the air by lowering the plate vibrations and the pressure wave radiation though the air at the peaks.

Finally, we point out the importance of the viscoelastic properties of the silicone rubber material used to achieve high STL values. In fact, some of the acoustic energy is converted into heat and lost by the contribution of this effect inside the rubber. In our study, we consider a fixed loss factor of 0.001 for the rubber, which allows reaching 86 dB of the STL obtained. In reality, the loss is higher in the conventional rubbers, with a factor of 0.01 and even 0.1. For these two values, the STLs at resonance are 62 dB and 42.6 dB, respectively, which remain high even at the realistic values of the loss factor of rubber. The reason of choosing 0.001 for the loss factor is mainly to emphasize the visibility, and then the existence of the two small peaks (β) and (γ).

4. Conclusion

We have provided a theoretical and numerical study to investigate the acoustic behavior of a plate-type acoustic metamaterial in an air-borne sound environment. Two configurations were considered, a spring-mass one and a pillar system-based one. We have shown that the considered metamaterial can produce a high STL in the sonic frequency range, which makes the system very suitable and effective for sound and vibration mitigation applications. In addition, we demonstrate that using well-chosen low-frequency resonators, the plate-type metamaterial can be a promising solution to overcome the

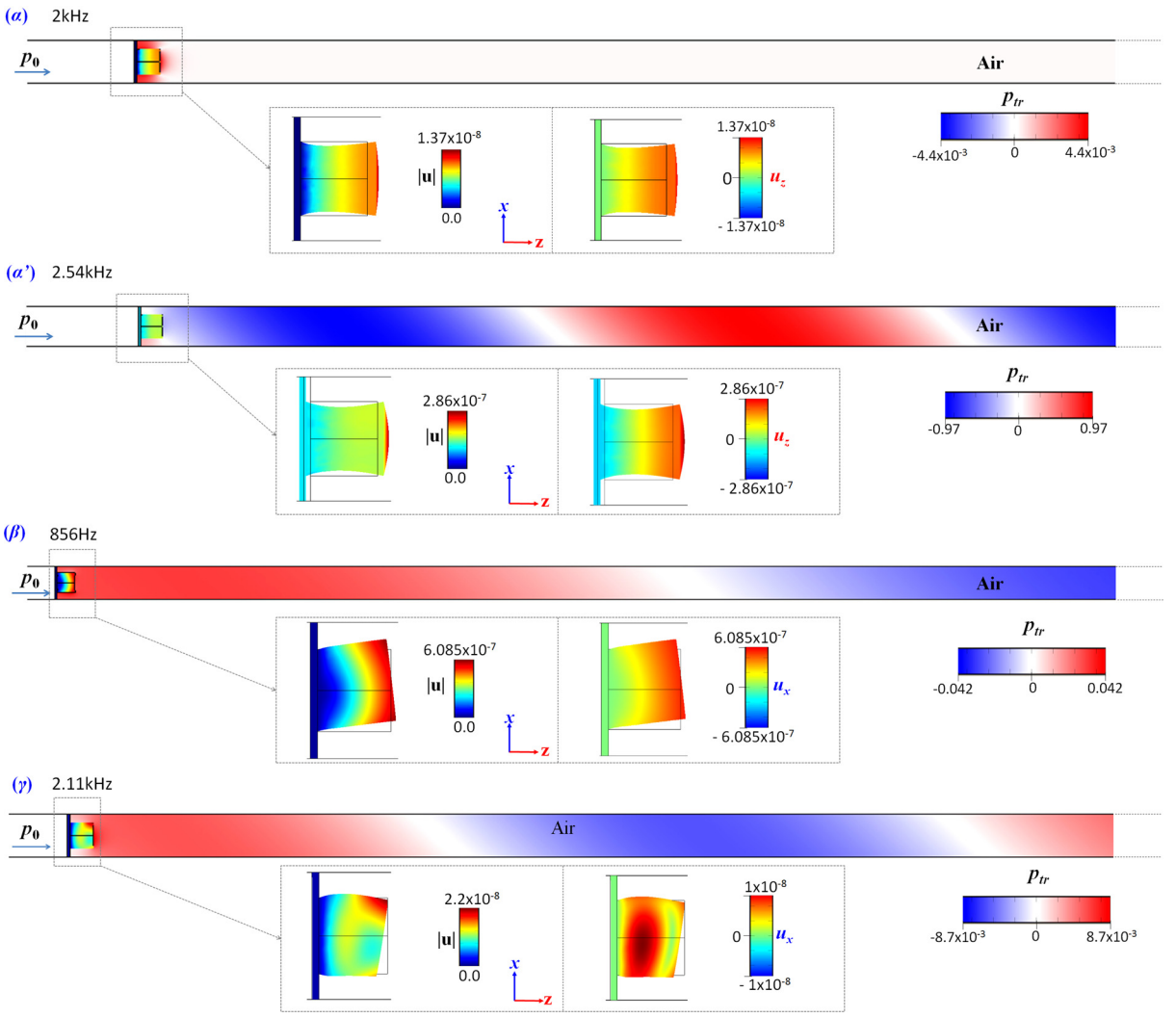

Fig. 5. Transmitted acoustic wave pressure and displacement field of the AM unit cell in specific picks and dips denoted in the STL curves by (α), (α'), (β) and (γ) in Fig. 4.

coincidence frequency limitation, which causes high sound transmission through plates for sound shielding. A physical understanding was provided and the associated mechanisms were discussed based on complete investigation and analysis including the air-borne sound approach (STL, displacement fields), the structure-borne results (band structure), and an effective mass density behavior.

Acknowledgements

This work was supported by the FEDER “Fonds européen de développement régional” (Project “MASTER”), the “Région Lorraine” and the PICS (France–China).

References

[1] S.S. Jung, Y.T. Kim, Y.B. Lee, S.I. Cho, J.K. Lee, J. Korean Phys. Soc. 53 (2008) 596.
[2] C.L. Dym, M.A. Lang, J. Acoust. Soc. Am. 56 (1974) 1523.
[3] Z. Qian, D. Chang, B. Liu, K. Liu, J. Vib. Acoust. 135 (2013) 061005.
[4] R. Zhou, M.J. Crocker, J. Sound Vib. 329 (2010) 673.
[5] K.-T. Chen, Appl. Acoust. 47 (1996) 303.
[6] V. Garcia-Chocano, S. Cabrera, J. Sanchez-Dehesa, Appl. Phys. Lett. 101 (2012) 184101.
[7] F. Asdrubali, Giulio Pispola, J. Acoust. Soc. Am. 121 (2007) 214.
[8] R.L. Mu, M. Toyodab, D. Takahashia, Appl. Acoust. 72 (2011) 849.
[9] Z. Liu, X. Zhang, Y. Mao, Y.Y. Zhu, Zh. Yang, C.T. Chan, Ping Sheng, Science 289 (2000) 1734.
[10] J. Li, C.T. Chan, Phys. Rev. E 70 (2004) 055602(R).

[11] Z. Liu, C.T. Chan, Ping Sheng, Phys. Rev. B 71 (2005) 014103.
[12] Y. Ding, Z. Liu, C. Qiu, J. Shi, Phys. Rev. Lett. 99 (2007) 093904.
[13] Y. Pennec, B. Djafari-Rouhani, H. Larabi, J.O. Vasseur, A.-C. Hladky-Hennion, Phys. Rev. B 78 (2008) 104105.
[14] Y. Pennec, B. Djafari Rouhani, H. Larabi, A. Akjouj, J.N. Gillet, J.O. Vasseur, G. Thabet, Phys. Rev. B 80 (2009) 144302.
[15] T.-T. Wu, Z.-H. Huang, T.-G. Tsai, T.-C. Wu, Appl. Phys. Lett. 93 (2008) 111902.
[16] M. Oudich, Y. Li, M.B. Assouar, Z. Hou, New J. Phys. 12 (2010) 083049.
[17] M. Oudich, M. Senesi, M.B. Assouar, M. Ruzenne, J.-H. Sun, B. Vincent, Z. Hou, T.-T. Wu, Phys. Rev. B 84 (2011) 165136.
[18] M.B. Assouar, M. Oudich, Appl. Phys. Lett. 100 (2012) 123506.
[19] M. Oudich, B. Djafari-Rouhani, Y. Pennec, M.B. Assouar, B. Bonello, J. Appl. Phys. 116 (2014) 184504.
[20] T.-C. Wu, T.-T. Wu, J.-C. Hsu, Phys. Rev. B 79 (2009) 104306.
[21] M. Oudich, M.B. Assouar, Z. Hou, Appl. Phys. Lett. 97 (2010) 193503.
[22] M.B. Assouar, M. Senesi, M. Oudich, M. Ruzzene, Z. Hou, Appl. Phys. Lett. 101 (2012) 173505.
[23] K.M. Ho, Z. Yang, X.X. Zhang, Ping Sheng, Appl. Acoust. 66 (2005) 751.
[24] J. Mei, G. Ma, M. Yang, Z. Yang, W. Wen, Ping Sheng, Nat. Commun. 3 (2012) 756.
[25] Y. Xiao, J. Wen, X. Wen, J. Sound Vib. 331 (2012) 5408.
[26] M. Oudich, X. Zhou, M.B. Assouar, J. Appl. Phys. 116 (2014) 193509.
[27] T. Still, M. Oudich, G.K. Auerhammer, D. Vlassopoulos, B. Djafari-Rouhani, G. Fytas, P. Sheng, Phys. Rev. B 88 (2013) 094102.